

Magnetotactic bacteria for cancer therapy

Cite as: J. Appl. Phys. **128**, 070902 (2020); <https://doi.org/10.1063/5.0018036>

Submitted: 15 June 2020 . Accepted: 27 July 2020 . Published Online: 17 August 2020

M. L. Fdez-Gubieda , J. Alonso , A. García-Prieto , A. García-Arribas , L. Fernández Barquín ,
and A. Muela 



ARTICLES YOU MAY BE INTERESTED IN

Antiferromagnetic spintronics

Journal of Applied Physics **128**, 070401 (2020); <https://doi.org/10.1063/5.0023614>

Ultrafast THz-driven electron emission from metal metasurfaces

Journal of Applied Physics **128**, 070901 (2020); <https://doi.org/10.1063/1.5142590>

Anisotropy in antiferromagnets

Journal of Applied Physics **128**, 040901 (2020); <https://doi.org/10.1063/5.0006077>

Lock-in Amplifiers
up to 600 MHz







Magnetotactic bacteria for cancer therapy

Cite as: J. Appl. Phys. 128, 070902 (2020); doi: 10.1063/5.0018036

Submitted: 15 June 2020 · Accepted: 27 July 2020 ·

Published Online: 17 August 2020



M. L. Fdez-Gubieda,^{1,2,a)}  J. Alonso,³  A. García-Prieto,^{2,4}  A. García-Arribas,^{1,2}  L. Fernández Barquín,³ 
and A. Muela^{2,5} 

AFFILIATIONS

¹Dpto. Electricidad y Electrónica, Universidad del País Vasco (UPV/EHU), 48940 Leioa, Spain

²BCMaterials, Basque Center for Materials, Applications and Nanostructures, UPV/EHU Science Park, 48940 Leioa, Spain

³Dpto. CITIMAC, Universidad de Cantabria, 39005 Santander, Spain

⁴Dpto. Física Aplicada I, Universidad del País Vasco (UPV/EHU), 48013 Bilbao, Spain

⁵Dpto. Inmunología, Microbiología y Parasitología, Universidad del País Vasco (UPV/EHU), 48940 Leioa, Spain

^{a)}Author to whom correspondence should be addressed: malu.gubieda@ehu.eus

ABSTRACT

Magnetotactic bacteria (MTB) are aquatic microorganisms that are able to biomineralize membrane-enclosed magnetic nanoparticles called magnetosomes. Inside the MTB, magnetosomes are arranged in a chain that allows MTB to align and navigate along the Earth's magnetic field. When isolated from the MTB, magnetosomes display a number of potential applications for targeted cancer therapies, such as magnetic hyperthermia, localized drug delivery, or tumor monitoring. The characteristics and properties of magnetosomes for these applications exceed in several aspects those of synthetic magnetic nanoparticles. Likewise, the whole MTB can also be considered as promising agents for cancer treatment, taking advantage of their self-propulsion capability provided by their flagella and the guidance capabilities ensured by their magnetosome chain. Indeed, MTB are envisaged as *nanobots* that can be guided and manipulated by external magnetic fields and are naturally attracted toward hypoxic areas, such as the tumor regions, while retaining the therapeutic and imaging capacities of the isolated magnetosomes. Moreover, unlike most of the bacteria currently tested in clinical trials for cancer therapy, MTB are not pathogenic but could be engineered to deliver and/or express specific cytotoxic molecules. In this article, we will review the progress and perspectives of this emerging research field and will discuss the main challenges to overcome before the use of MTB can be successfully applied in the clinic.

© 2020 Author(s). All article content, except where otherwise noted, is licensed under a Creative Commons Attribution (CC BY) license (<http://creativecommons.org/licenses/by/4.0/>). <https://doi.org/10.1063/5.0018036>

INTRODUCTION

Cancer is one of the most common causes of death worldwide. According to the Global Cancer Observatory,¹ only in 2018, around 18.1×10^6 new cases were reported, with a mortality rate higher than 50%. These statistics reflect the need of finding novel strategies and more effective cancer treatments that substitute or complement the current ones, namely, surgery, chemotherapy, radiotherapy, and immunotherapy. These new strategies should overcome the known limitations that are inherent to standard treatments, such as unspecific targeting, shallow penetration of electromagnetic fields, heterogeneous distribution in the tumor area, and non-selective cytotoxicity. The visionary speech delivered by Richard Feynman in 1959,² which anticipated numerous technological advances that are ubiquitous nowadays, also introduced the

idea of using small machines as robotic surgeons. These should be capable of navigating through the vascular system of the body, specifically, finding the damaged cells or organs and performing locally the therapeutic action. Aiming to materialize what would be an extraordinary therapeutic tool, different kinds of systems acting as nanorobots have been investigated in laboratories across the world.³ A significant number of them are based on biological entities such as bacteria and viruses^{4–6} and many others on inorganic magnetic nanoparticles (MNPs).^{7,8}

MNPs engineered for biomedical applications are, in the simplest case, composed of a single core magnetic nanoparticle, usually an iron oxide, surrounded by a biocompatible shell. The diameter of the nanoparticles is tuned in the range between 5 and 50 nm, a size that is suitable for the interaction with biological entities and enables their penetration into cells. In the last decades, much of the

work has been focused on magnetite (Fe_3O_4) and maghemite ($\gamma\text{-Fe}_2\text{O}_3$), due to their good biocompatibility⁹ and their relatively high magnetic susceptibility and saturation magnetization, resulting in a high response to external magnetic fields. In addition, they are currently the only FDA (US Food and Drug Administration) and EMA (European Medicines Agency) approved magnetic materials for biomedical treatment.

In this sense, a great effort has been carried out to design MNPs for specific applications addressing cancer diseases, such as magnetic hyperthermia, targeted drug delivery, and detection of cancer cells.^{7,10,11} In magnetic hyperthermia therapy, MNPs are injected into the tumor and heated by an external alternating magnetic field (AMF). Under the AMF, the magnetic response of the MNPs describes a hysteresis loop, whose area is proportional to the dissipated energy, producing an elevation of the temperature in the tumor. A local increase in temperature, around 4–7 °C, drives cancer cells to apoptosis without affecting the healthy ones. The use of MNPs in cancer therapy through magnetic hyperthermia has been authorized in Europe since 2011, as a co-adjuvant therapy with conventional radio- and chemotherapies for the treatment of brain tumors. In 2014, the FDA also approved this procedure for the treatment of glioblastoma and prostate cancer. Currently, clinical trials are being carried out by MagForce AG¹² on patients with brain, pancreatic, prostate, breast, and esophageal cancer (see Table I). Alternatively, MNPs are also investigated for targeted drug delivery purposes. The main goal is to properly functionalize the surface of the nanoparticle with a specific drug and, through the application of an external magnetic field gradient, to transport the MNPs toward the tumor tissue.¹³ Even though a large number of *in vivo* and *in vitro* studies have been performed, there are no ongoing clinical trials so far. MNPs are also used for tumor localization and imaging. A recent example of the success of MNPs for tumor localization is the application developed by Endomag[®],¹⁴ where a combination of MNPs (Table I) and a high resolution sensor (Sentimag) is used to detect and follow the evolution of breast cancer. MNPs for imaging are employed in the well-established application of Magnetic Resonance Imaging (MRI) as contrast enhancement agents, for example, in liver visualization.¹⁵

TABLE I. Currently approved MNPs for cancer clinical purposes.

Magnetic nanoparticles (MNPs)	Indication
Nanotherm: Aminosilane coated iron oxide MNP-	Magnetic hyperthermia ^a
Sienna+: Dextran-coated iron oxide MNPs	Tracer for cancer locating lymph nodes ^b
Resovist [®] : Dextran-coated iron oxide MNPs	MRI imaging of the liver ^c

^aManufactured by Magforce; Classification (Council Directive 93/42/EEC) as a class III medical device.

^bManufactured by Endomag[®] Ltd; Classification (Council Directive 93/42/EEC) as a class IIa medical device.

^cManufactured by Fujifilm RI Pharma; Classification (Council Directive 93/42/EEC) as a drug.

Unfortunately, there are several intrinsic limitations associated to the use of MNPs as nanorobots. These include their limited penetration through biological barriers, poor reaching and targeting capacity, and uneven distribution in the tumor tissue. In order to bypass these and other difficulties, different alternatives have been proposed in the last few years. Among them, the idea of using biological entities such as viruses and bacteria to interact with tumors has been gaining momentum.

Bacteria have a long history in cancer therapy. Already in 1890, Coley¹⁶ discovered that some cancer patients recovered after suffering bacterial infections that destroyed the tumors. Over the past century, many genera of bacteria have been investigated as anticancer agents.⁶ The effectiveness of bacteria against cancer relies upon their ability to selectively infect and kill the cancer cells *in situ*. Motility is one of the key features of bacterial therapy, since bacteria can actively swim and penetrate deep into the tumor tissue. It happens that tumors display irregular and chaotic vasculature, leading to areas with low oxygen concentration and nutrient limitation.¹⁷ Such hypoxic regions are a perfect niche for anaerobic and microaerophilic bacteria to perform selective colonization. The mechanism behind this bacterial therapy is still not well understood, but there is evidence indicating that bacteria could perform direct oncolysis and stimulate the immune system.⁶ Direct oncolysis is mediated by secreting exotoxins in the tumor area and by competing for nutrients. In addition, bacterial infections activate the immune system, which targets not only bacteria but also tumor cells. Another advantage of bacterial therapy is that the bacteria can be genetically modified to deliver and/or express specific cytotoxic agents, increasing their effectiveness. In the last years, the FDA has allowed several clinical trials with tumor-targeting bacteria, and these human studies show promising antitumor activities (see Table II). Despite this, so far the only established standard of medical care with bacteria is the treatment of superficial bladder cancer using Bacillus Calmette-Guerin (BCG).¹⁸

Patients are treated with either intravenous or intratumoral administration, with only one dose or dose escalation, depending on the trial. In the particular case of *Mycobacterium* and bladder cancer, patients receive repeated instillations of live bacteria into the bladder. During systemic administration, bacteria disseminate either in tumor or in healthy tissues. However, a selective colonization of the tumor occurs as a consequence of the immunosuppressive and biochemically special microenvironment.^{19–22}

Unfortunately, up to now, the bacteria tested in clinical trials cannot be guided or tracked inside the body by using external devices. It is for this reason that a particular group of bacteria, namely, *magnetotactic bacteria* (MTB), stand out as a promising paradigm of bacterial cancer therapy. This is because, as will be shown in this work, MTB naturally synthesize MNPs, thereby merging the guidance, control, and therapeutic capabilities of MNPs with motility, chemical specificity, and the capacity of being genetically modified of bacteria.

MAGNETOTACTIC BACTERIA (MTB)

The magnetotactic behavior in bacteria was first observed by Salvatore Bellini (1963)²³ in freshwater samples. He observed bacteria swimming northward persistently and suggested the presence of

TABLE II. Bacterial species tested in clinical trials for cancer therapy.^a

Bacteria species	Cancer type	Clinical trial phase
<i>Mycobacterium bovis</i>	Bladder cancer	1, 2, and 3
	Prostate cancer	
	Lung cancer	
	Melanoma	
	Metastatic colorectal cancer	
<i>Listeria monocytogenes</i>	Pancreatic cancer	1 and 2
	Prostatic neoplasms	
	Colorectal neoplasm	
	Metastatic pancreatic cancer	
	Lung carcinoma	
<i>Salmonella Typhimurium</i>	Cervical cancer	1
	Head and neck cancer	
	Oropharyngeal carcinoma	
<i>Clostridium novyi</i>	Neoplasm metastasis	1
	Unspecific solid tumor	
	Liver cancer	
<i>Bifidobacterium longum</i>	Biliary cancer	1
	Solid tumors	
	Malignant neoplasm of lung breast, digestive organs, urinary tract, brain, endocrine glands, and genital organs	

^aData obtained from ClinicalTrials.gov database (<https://clinicaltrials.gov>). The phase is based on the study's objective, the number of participants, and other characteristics. There are five phases: early phase 1 (formerly listed as phase 0), phase 1, phase 2, phase 3, and phase 4.

an internal magnetic compass responsible for their orientation. More than 10 years later, Blakemore in 1975²⁴ discovered bacteria in marine sediments swimming along the geomagnetic field lines, and by using transmission electron microscopy, he observed intracellular magnetic organelles aligned forming a chain inside the bacteria. R. P. Blakemore referred to the magnetic organelles as *magnetosomes* and classified the bacteria as *magnetotactic bacteria*, MTB.

MTB are aquatic motile microorganisms ubiquitous in marine and freshwater environments.²⁵ They can passively align, Fig. 1(a), and actively swim along the geomagnetic field lines, Fig. 1(b), due to the presence of one or more chains of magnetosomes positioned along the longitudinal axis of the cell.^{26–29} This behavior is known as *magnetotaxis*.

MTB are microaerobic/anaerobic microorganisms easily found in the oxic–anoxic transition zones (OATZs) [Fig. 1(b)] with vertical chemical gradients. MTB have sensory elements that guide them to the regions with their preferred oxygen concentration, an ability called *aerotaxis*. Given these circumstances, magnetotaxis is a great advantage to search their nutritional requirement.²⁶ The geomagnetic field lines act as a pathway for searching the optimal position in the stratified water column, since bacteria aligned in the Earth's magnetic field reduce a three-dimensional search to a single

dimension. Moreover, other possible roles of the magnetosomes have also been suggested, such as acting as detoxifying agents, capable of scavenging metal ions, or reactive oxygen species.^{32,33}

All MTB described at present show great morphological and physiological diversities. The described morphotypes include [see Fig. 2 (top)] curved (a), spirilla (b), cocci (c), rods (d), and even some colonial bacteria, which form multicellular aggregates.^{29,34} The only common signature is the capability to swim along magnetic field lines, including the Earth's magnetic field.

Regarding magnetosomes, two structures can be differentiated, the mineral magnetic core and an organic envelope that consists of a proteinaceous lipid bilayer membrane.^{18,27,28} The mineral core presents high chemical purity, being magnetite, Fe₃O₄, in most of the species, though some of them synthesize greigite, Fe₃S₄. The composition, morphology, and size of the magnetosomes are characteristics of each species. This fact clearly reflects that the formation of magnetosomes is driven by a strict genetic control.³⁹ On the other hand, the morphologies of the crystals can be [see Fig. 2 (bottom)] cube-octahedral (a), elongated prismatic [(b) and (c)], and bullet- or tooth-shaped [(d) and (e)]. Finally, the size of the magnetic crystals ranges between 35 and 120 nm. Interestingly, in this diameter range, MNPs are room-temperature stable single-magnetic domains,^{26,29,40–43} see Fig. 1(c). The arrangement of the magnetosomes in a chain causes the addition of magnetic moments of every individual magnetosome, turning the cell into a single magnetic dipole, Fig. 1(d). Obviously, this allows MTB to behave as compass needles that passively get aligned along magnetic field lines.^{40,44,45}

MTB are microorganisms difficult to grow and maintain in the laboratory,²⁵ and until now, only a few species have been isolated in axenic culture and deposited in bioresource centers. The first isolated species from freshwater sediments were *Magnetospirillum gryphiswaldense* MSR-1, Fig. 3(a), and *Magnetospirillum magneticum* AMB-1,^{46,47} Fig. 3(c), in the early 1990s. Both are spirilla and biomineralize cube-octahedral magnetite crystals arranged in a single chain, Figs. 3(b) and 3(d). These strains are easy to culture, and most of the recent laboratory work has been carried out with them. Alternatively, *Magnetovibrio blakemorei* MV-1,⁴⁸ Fig. 3(e), is a marine vibrioid to helicoid morphotype that biosynthesizes elongated magnetite nanoparticles with a crystal morphology described as truncated hexa-octahedral, Fig. 3(f). Various research groups have been involved on the mass cultivation of MTB strains.^{49–54} The culture media composition and the incubation conditions have been optimized to increase the growth yield (Y_{cel}) and magnetosome production (Y_{mag}) mainly in *M. gryphiswaldense* MSR-1 and *M. magneticum* AMB-1. Up to now, the highest values have been reported for MSR-1, Y_{cel} of 9.16 g/l and Y_{mag} of 356 mg/l.⁴⁹

Currently, the potential of magnetosomes for biomedical applications is being widely studied as an alternative to synthetic MNPs. In fact, magnetosomes are good candidates not only because of their chemical purity and well-defined morphology and size in the stable magnetic monodomain range, but also because they are surrounded by a biocompatible organic envelope that confers them stability when dispersed in water and facilitates the attachment of bioactive molecules.^{55–58} However, in the last years, seizing the advantage of the self-propulsion capability of MTB provided by their flagella and the presence of the magnetosome chain,

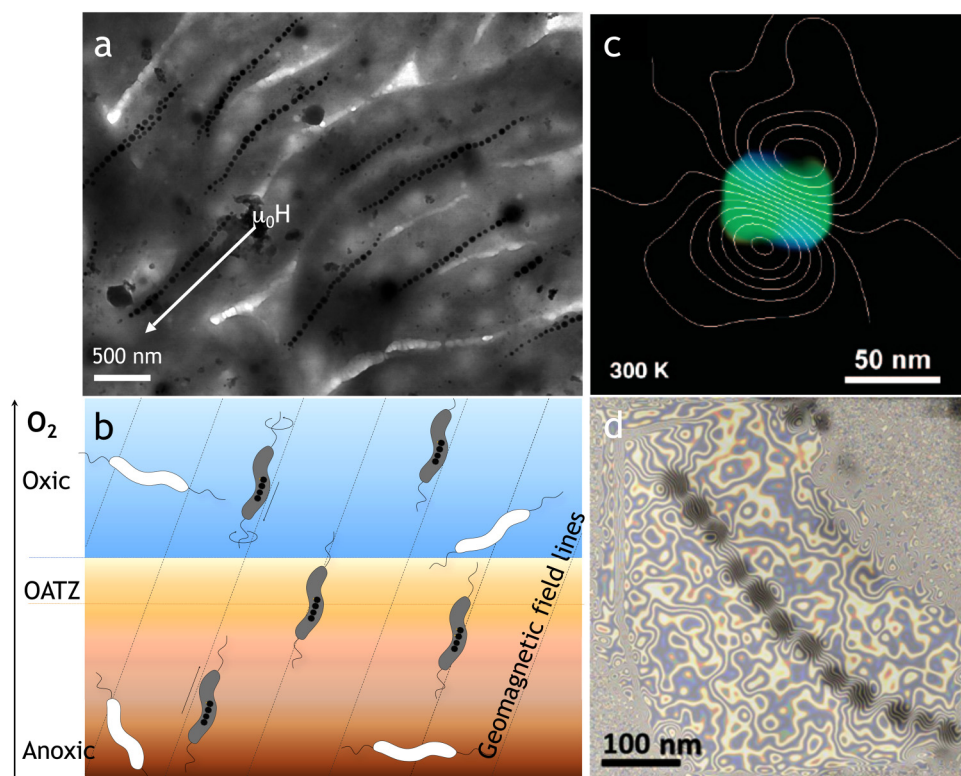


FIG. 1. Magnetotaxis behavior. (a) Transmission electron microscope image (TEM) of *Magnetospirillum gryphiswaldense* under an external magnetic field of 0.5 T. The white arrow marks the direction of the applied field. (b) Schematic representation of magnetotaxis in the oxic-anoxic transition zone (OATZ) (Courtesy of Dr. Lourdes Marcano). Electron holography of (c) an isolated magnetosome [reproduced with permission from Thomas *et al.*, Acc. Chem. Res. **41**, 665 (2008). Copyright 2008 American Chemical Society] and (d) a chain of isolated magnetosomes [reproduced from Huizar-Félix *et al.*, Appl. Phys. Lett. **108**, 063109 (2016). Copyright 2016 AIP Publishing LLC].

recent works have focused on the use of the whole MTB as a biomedical agents. MTB are envisaged as *nanobots* that can be guided and manipulated by external magnetic fields and are naturally attracted toward hypoxic areas such as the tumor regions. Unlike most of the bacteria currently tested in clinical trials for cancer therapy (Table II), MTB are not pathogenic but could be engineered to deliver and/or express specific cytotoxic molecules. Moreover, the presence of magnetosomes provides the MTB with biomedical capacities for therapy and imaging attributed to them, such as the ability to heat up under alternating magnetic fields for magnetic hyperthermia therapy, avoiding the tedious and low efficient process needed to isolate the magnetosomes from the MTB. Figure 4 summarizes the advantages and perspectives of MTB as potential theranostic agents that will be discussed in the following sections.

MAGNETOTACTIC BACTERIA AS MAGNETIC HYPERTHERMIA AGENTS

Since Gilchrist *et al.*⁵⁹ demonstrated in 1957 that magnetic particles could be inductively heated to kill lymphatic metastases, magnetic hyperthermia has become one of the most promising emerging techniques for cancer therapy.^{9,60–62} As mentioned before, by increasing the temperature of the tumor area up to 42–45 °C, the so-called therapeutic window, cancer cells can eventually be led to apoptosis.⁶¹ Higher temperatures, >50 °C, would lead to a more disruptive (and less safe) destruction of the cancer cells, through thermal ablation.⁶³ In addition, it has been observed

that raising the temperature in the tumor improves the efficiency of adjuvant therapies, such as chemotherapy and radiotherapy.⁶⁴

A huge research effort has been focused on maximizing the heating efficiency of MNPs. Higher heating efficiencies will ensure lower dosages of MNPs to efficiently increase the temperature in the tumor area, reaching the desired therapeutic window under a certain AMF. The efficiency is parametrized by a magnitude defined as *Specific Absorption Rate* (SAR)^{65,66} that can be determined from the initial slope of the heating curves, $\Delta T/\Delta t$, recorded during the magnetic hyperthermia treatment [Fig. 5(a)] through the following equation:

$$\text{SAR} \left(\frac{W}{g} \right) = \frac{m_s}{m_n} C_p \frac{\Delta T}{\Delta t}, \quad (1)$$

where C_p is the specific heat of the solvent, m_s is the mass of the solvent, and m_n is the mass of the MNPs. In addition, since the heating efficiency of MNPs is proportional to the magnetic energy losses or the area of the AC hysteresis loop [Fig. 5(b)], the SAR values can also be obtained from the following equation:⁶⁶

$$\text{SAR} \left(\frac{W}{g} \right) = \frac{f}{c} \cdot A = \frac{f}{c} \cdot \oint \mu_0 M_t dH_t, \quad (2)$$

where M_t is the instantaneous magnetization at time t , H_t is the amplitude of the oscillating magnetic field of frequency f at time t , and c is the weight concentration of MNPs in the medium.

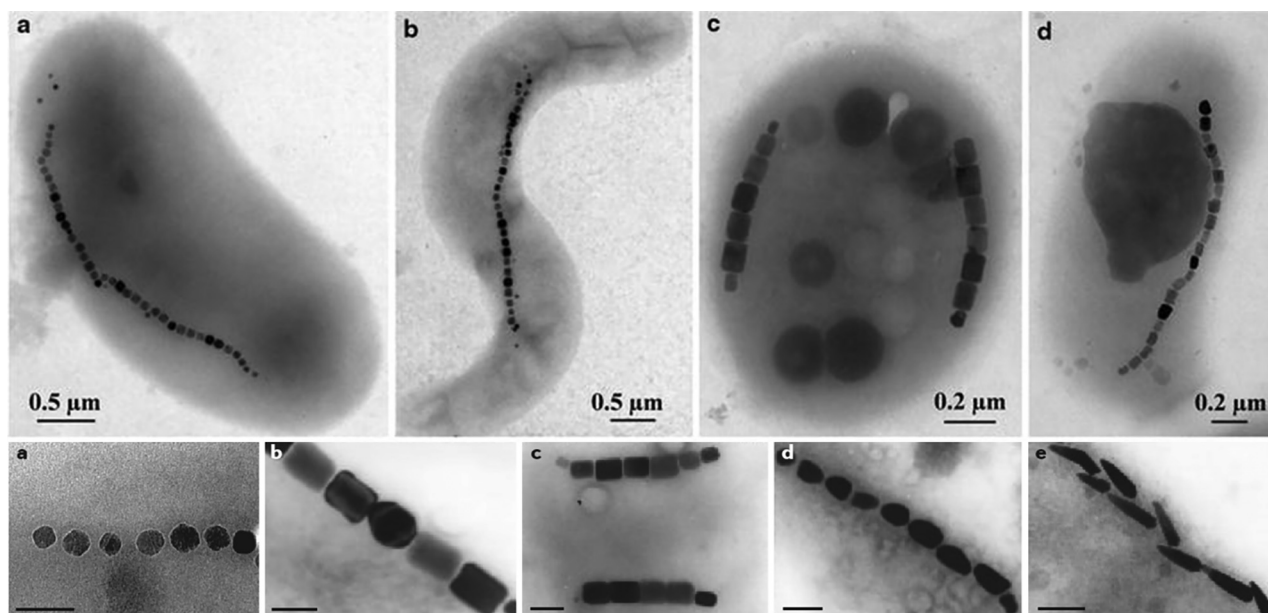


FIG. 2. TEM images of MTB and magnetosomes. Top: Different morphotypes of bacteria: (a) curved, (b) spirilla, (c) cocci, and (d) rod. Adapted with permission from Bazylinski *et al.*, *The Prokaryotes—Prokaryotic Physiology and Biochemistry*. Copyright 2013 Springer Nature. Bottom: Crystal morphologies: (a) cube-octahedral, (b) and (c) elongated prismatic, (d) tooth-shaped, and (e) bullet-shaped. Scale bars, 100 nm. Adapted with permission from Uebe and Schüler, *Nat. Rev. Microbiol.* **14**, 621 (2016). Copyright 2016 Springer Nature.

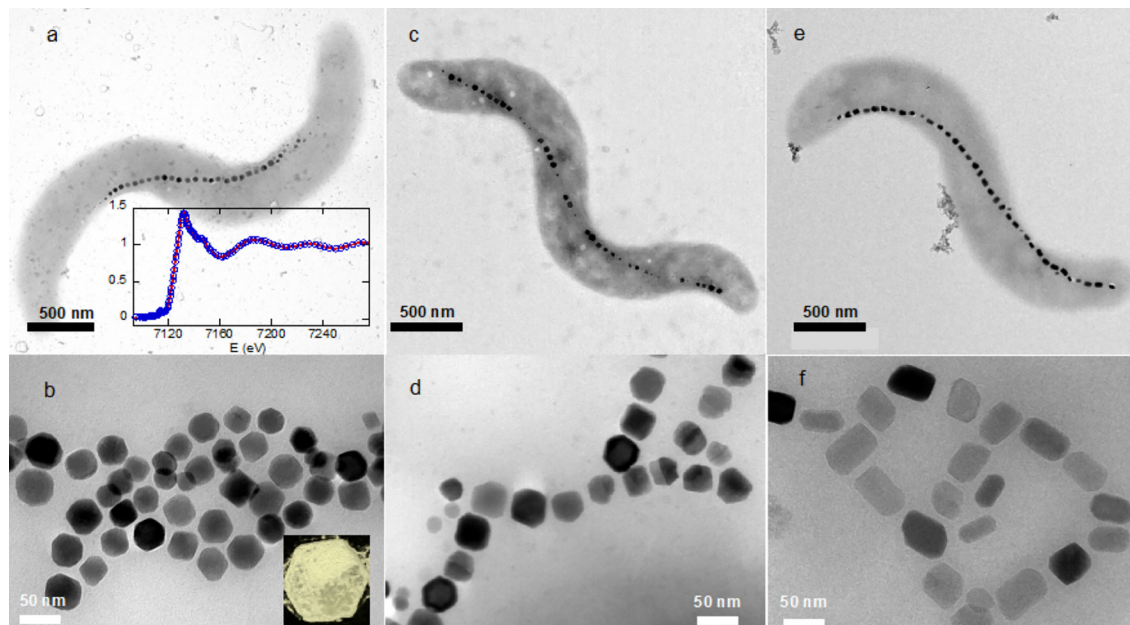


FIG. 3. Transmission electron microscopy of (a) *M. gryphiswaldense* [inset: x-ray absorption near-edge spectroscopy (XANES) spectra of MTB (red) compared to magnetite (blue)]; (b) isolated cube-octahedral magnetosomes of (a) (inset: Cryo-electron tomographic image of a single magnetosome); (c) *M. magneticum*; (d) isolated cube-octahedral magnetosomes of (c); (e) *M. Blakemorei*; and (f) isolated hexo-octahedral magnetosomes of (e).

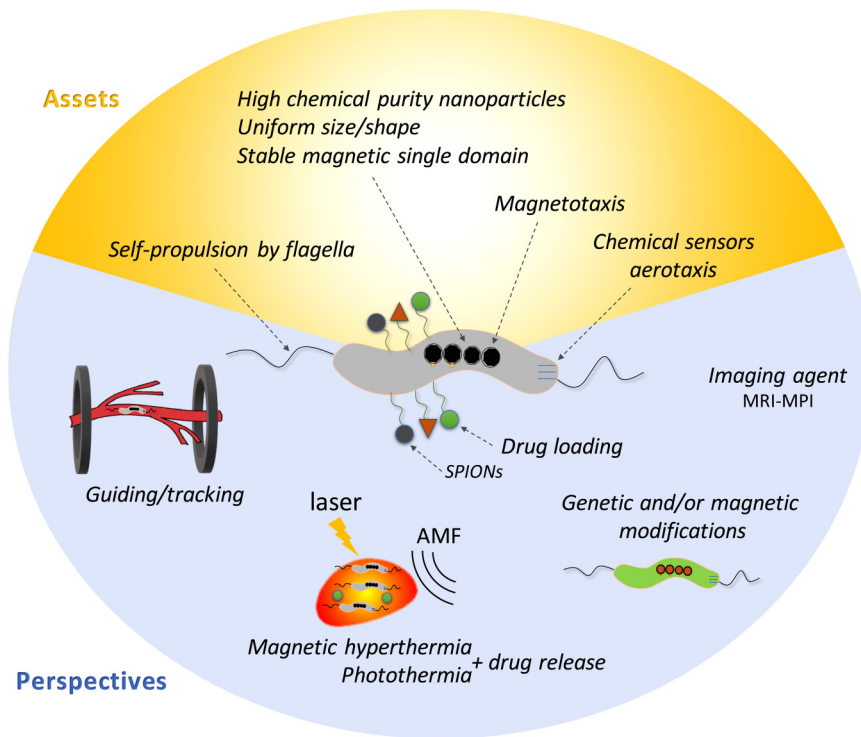


FIG. 4. Schematic representation of the biological mechanisms of MTB that envisage them as promising nanobots, and the perspectives of the use of MTB as theranostic agents for cancer treatments.

Considering the definition of SAR, there are different parameters that can be tuned to maximize SAR values. On the one hand, there are external parameters such as the amplitude and frequency of the magnetic field, and the dosage of MNPs. On the other hand, we have the intrinsic magnetic properties of MNPs such as magnetic anisotropy and spontaneous magnetization. External parameters are currently limited by technical, medical, and economical factors.^{9,60,61} For example, high-frequency magnetic fields may generate eddy currents

that can be harmful to the patient. Therefore, in clinical trials, the values of the amplitude, H , and frequency, f , of the AMF are limited to values in which the effects of the eddy currents are within safety limits for the patient.^{67,68}

Due to these technical/medical limitations, most of the research has been focused on improving the intrinsic magnetic properties of MNPs. Since SAR is proportional to the area of the hysteresis loop, we look for tuning those parameters that control

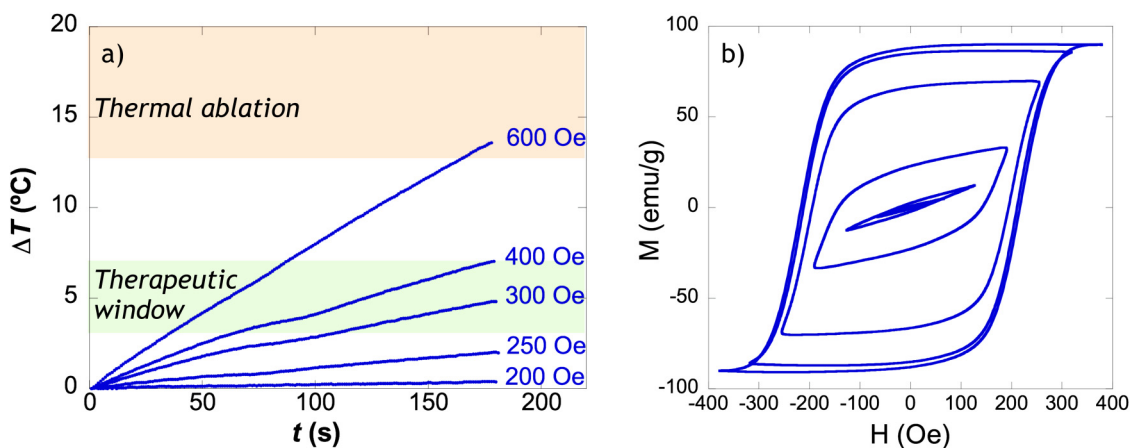


FIG. 5. (a) Heating curves, ΔT_{emp} vs time, and (b) AC hysteresis loops, M vs H , of *M. gryphiswaldense* dispersed in water (measured at 300 kHz).

the area of the loop, fundamentally, the magnetic anisotropy and the saturation magnetization. Two main strategies have been used for this purpose, controlling the size and shape of the MNPs^{69–73} and modifying their composition.⁷⁴ To this respect, most of the research studies performed so far have been focused on superparamagnetic iron oxide-based nanoparticles (SPIONs).⁷⁵ The smallest sizes (<15–20 nm) of SPIONs were, in principle, considered more adequate for *in vivo* applications.⁷⁶ However, SPIONs present a series of drawbacks for magnetic hyperthermia, especially a thermally unstable magnetic moment at the body temperature. This can result in subpar magnetic properties and relatively poor heating efficiency. Therefore, in recent years, different groups have investigated the use of bigger MNPs (≈ 20 –50 nm). Magnetite nanoparticles in this size range and, in particular, magnetosomes from MTB are single magnetic domains that are stable at room temperature, providing higher hysteresis losses and consequently higher SAR values.^{70,77,78} For these larger MNPs, the evolution of SAR as a function of the magnetic field is explained accurately by a modified Stoner–Wohlfarth model.^{58,79,80} The general behavior is well described in Fig. 6(a) for isolated magnetosomes from *M. gryphiswaldense*: at low magnetic field amplitudes, the SAR value is small, whereas above a threshold field, the SAR exhibits a rapid increase, tending to saturate at high magnetic field amplitudes.

The use of magnetosomes for *in vitro* and *in vivo* hyperthermia treatment has already been tested with very promising results.^{56,58,82–84} In a recent work, mice bearing xenografted MDA-MB-231 breast cancer were treated with chains of magnetosomes from *M. magneticum* AMB-1, under a magnetic field of $H = 200$ Oe and $f = 198$ kHz, leading to the total disappearance of tumor after 30 days.⁸⁵ In another work, magnetosomes coated with poly-L-lysine were administered to mice with glioblastoma.⁸⁶ The mice were exposed to 27 magnetic hyperthermia sessions, each lasting 30 min, using a magnetic field of $H = 270$ Oe and $f = 202$ kHz. All of the mice were alive and apparently cured 350 days after the first injection. In addition, it has been shown that

these magnetosomes are capable of maintaining anti-tumor activity even after suffering high levels of degradation inside the tumor cells, which makes them ideal candidates for long-term hyperthermia treatment.⁸⁷

However, the delivery method of MNPs, in general, and magnetosomes, in particular, to the tumor area is mainly limited nowadays to direct intra-tumoral injection, which is only suitable for well-localized tumors (e.g., prostate), being the procedure invasive.⁸⁸ Ideally, indirect administration methods, such as intravenous or intra-arterial, would be more desirable, but in these cases, generally fewer MNPs end up reaching the tumor.^{89,90} To this respect, MTB present as compelling candidates for magnetic hyperthermia. Besides their self-propelling capacity and the possibility to guide and track them, the chain configuration of magnetosomes maximizes their heating efficiency^{81,91} in comparison to randomly arranged nanoparticles, and the chain being anchored inside the bacteria prevents the agglomeration of the magnetosomes in the tumor, a fact that would decrease their heating efficiency.

One of the first studies on the heating efficiency of the whole MTB was carried out by Alphandery *et al.* in 2011.^{85,92} In that work, the authors compared the heating efficiency of individual magnetosomes, magnetosome chains extracted from MTB, and the whole MTB. The results revealed a much higher heating efficiency from MTB than from extracted chains and individual magnetosomes. In 2017, Tabatabaei *et al.*⁹³ proposed the use of MTB with attached commercial SPIONs as heat delivering agents to open the blood–brain barrier for brain tumor treatment. In a more recent work, Gandia *et al.*⁸¹ studied the heating efficiency of MTB and compared the results with those obtained by isolated magnetosomes. A combination of calorimetric and magnetometric methods was employed to analyze the heating efficiency. The heating efficiency of MTB was measured at AMFs between $H = 0$ –600 Oe and $f = 150$ –530 kHz under different bacterial configurations: randomly and parallel aligned (in the viscous medium) and randomly dispersed (in water), see Fig. 6(b). Independent of the configuration,

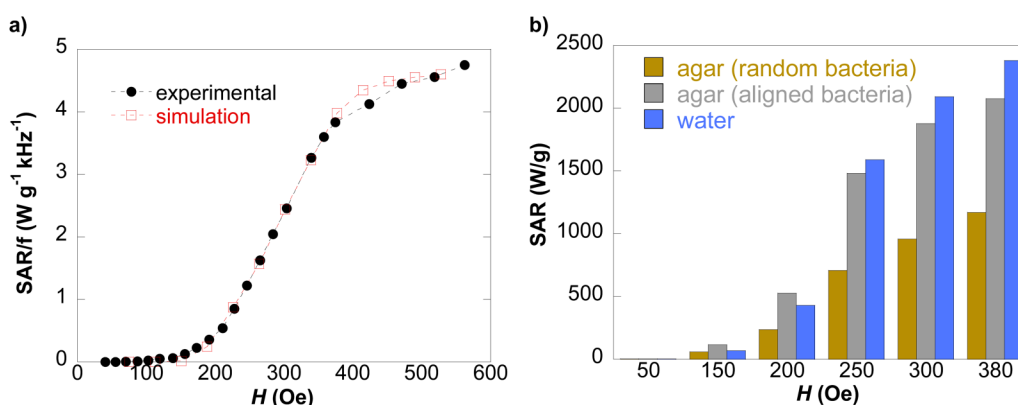


FIG. 6. (a) Experimental SAR normalized by the frequency, SAR/f , measured at $f = 150$ kHz of isolated magnetosomes of *M. gryphiswaldense*. The simulated curve for SAR/f , calculated using the Stoner–Wohlfarth model is also included for comparison. Reproduced with permission from Muela *et al.*, *J. Phys. Chem. C* **120**, 24437 (2016). Copyright 2013 American Chemical Society. (b) SAR values obtained from hysteresis loops of MTB under different configurations. Measurements were carried out at $f = 300$ kHz. Reproduced with permission from Gandia *et al.*, *Small* **15**, 1902626 (2019). Copyright 2019 John Wiley & Sons.

TABLE III. Heating efficiency of isolated magnetosomes and MTB dispersed in water. Considering that, for MTB, the SAR vs magnetic field curve tends to start saturating above $H = 300\text{--}400$ Oe, for a proper comparison, in Table III, we have included SAR values reported for $H > 300$ Oe.

	Amplitude (Oe)	Frequency (kHz)	Concentration (mg/ml)	SAR (W g^{-1})	SAR/f ($\text{W g}^{-1} \text{kHz}^{-1}$)	Reference
<i>M. gryphiswaldense</i> MSR-1	380	310	0.15	2380	7.7	81
<i>M. magneticum</i> AMB-1	880	108	0.45	864	8.0	92
Isolated magnetosomes of MSR-1	380	310	0.2	1428	4.4	58
Isolated magnetosomes of AMB-1	800	183	1.0	400	2.2	87
Isolated magnetosomes of AMB-1 doped with Co	800	183	1.0	500	2.7	87
Magnetite nanocubes	600	310	1.0	712	2.3	70

the therapeutic window could be reached in less than 5 min. With the increasing magnetic field, the SAR vs H curves described the typical Stoner–Wohlfarth behavior, with nearly null values for $H < 150$ Oe, and a steep increase afterward, tending to saturate for $H > 300$ Oe, where the AC loops showed a shape close to the optimum shape expected for an ideal heating mediator (i.e., rectangular loops with high squareness). Due to the anisotropic nature of the magnetosome chain, the heating efficiency was maximized when the bacteria were aligned parallel to the applied magnetic field. Nevertheless, the heating results obtained with the randomly dispersed MTB were still better than those typically reported for MNPs and closer to those obtained in the case of isolated magnetosomes, see Table III. Therefore, it is clear that the alignment plays an important role in the heating efficiency of MTB. In addition, the fact that the loops of the MTB dispersed in water resemble those of oriented MTB in the viscous medium indicates that physical rotation or Brownian relaxation plays nearly no role in the heating efficiency of MTB.⁹⁴ This feature suggests that, contrary to what frequently happens with inorganic MNPs, MTB will still be able to provide high heating efficiency after penetrating and getting immobilized inside the tumor. Moreover, since the MTB end up being internalized or attached to the cancer cells, local heating effects can give rise to deactivation of the cancer cells even if there was no global rise in the temperature of the medium.

Nowadays, a few *in vitro* or *in vivo* hyperthermia tests have been carried out with MTB in cancer cell lines and tumors in experimental animals. Gandia *et al.*⁸¹ assayed MTB with human lung A549 carcinoma cells. After 24 h of contact, SEM and transmission electron microscope (TEM) images showed the presence of MTB adhered to or internalized by the cancer cells, Figs. 7(a)–7(c). Cancer cells loaded with MTB were subjected to an AMF of $H = 400$ Oe and $f = 150$ kHz during 45 min. An immediate effect was observed after the treatment: the growth of cancer cells drastically slowed down, and at the end of the experiment, the number of living cancer cells was three times lower than the control, Fig. 7(d). In previous studies, *in vivo* magnetic hyperthermia was tested with MTB inside mice by Alphandery *et al.* in 2011.⁸⁵ However, no antitumoral activity was observed, which was attributed to the low temperature increase measured in the tumor area due to the low bacterial doses employed. Additionally, in parallel, Chen *et al.* in 2016,⁹⁵ studied the use of MTB to kill *Staphylococcus aureus* via magnetic hyperthermia. *S. aureus* is a pathogen that causes skin and soft tissue infections, and the authors reported that MTB could effectively kill $\sim 50\%$ of *S. aureus*.

MAGNETOTACTIC BACTERIA FOR TARGETED THERAPIES

A major challenge in cancer therapy is to deliver efficiently the therapeutic agent to the target site to minimize side effects. In this line, the use of MNPs stands out as an emerging technology that has been extensively studied in the last years.^{11,13} The idea behind it is to attract the MNPs to the region of interest with the use of magnetic field gradients. For successful targeting, MNPs will need to counteract the drag and buoyancy forces of the fluid with a magnetic force that depends on the field gradient and the magnetic moment of the MNP,⁹⁶ so that, for a given field gradient, the force is maximum at saturation. In the case of SPIONs, saturation only occurs at high fields, and producing the field strengths and field gradients necessary to control the movement of the MNPs in deep tissues is challenging, especially when platforms need to be scaled up to the clinical size.^{3,11}

In this context, MTB present a number of advantages against MNPs that make them good candidates to implement therapy strategies locally addressed at the tumor site such as targeted drug-delivery or magnetic hyperthermia. Indeed, MTB have self-propulsion capabilities provided by their flagella, and the magnetic moment of the magnetosome chain, made up of the sum of those of the individual magnetosomes, is high enough to allow the MTB to passively align along magnetic fields as small as the Earth's ($\approx 50 \mu\text{T}$) in water environments. MTB swim along the magnetic field lines (magnetotaxis), and therefore, no magnetic field gradients are necessary to guide them. The navigation of the MTB can be controlled by torque-based actuation on the magnetosome chain, which requires less magnetic field strength than the pulling approaches necessary for MNPs.³ In addition to magnetotaxis, the navigation direction of the bacteria is also driven by the oxygen gradients present in the medium (aerotaxis) which favor their preference for hypoxic regions such as those in the tumors.

However, the possibility of application of remotely guided bacteria to real clinical cases is still in its very early development. Preliminary works in this field have shown that *M. magneticum* can navigate in capillaries and target mouse tumor xenografts⁹⁷ and that *Magnetococcus marinus* carrying drug-loaded nanoliposomes [Fig. 8(a)] can be magnetically guided toward hypoxic regions of colorectal xenografts.⁹⁸ Here, 55% of the injected MTB penetrated into the hypoxic regions of the tumor, which was a large improvement in comparison to the targeting efficiency of other nanocarriers.

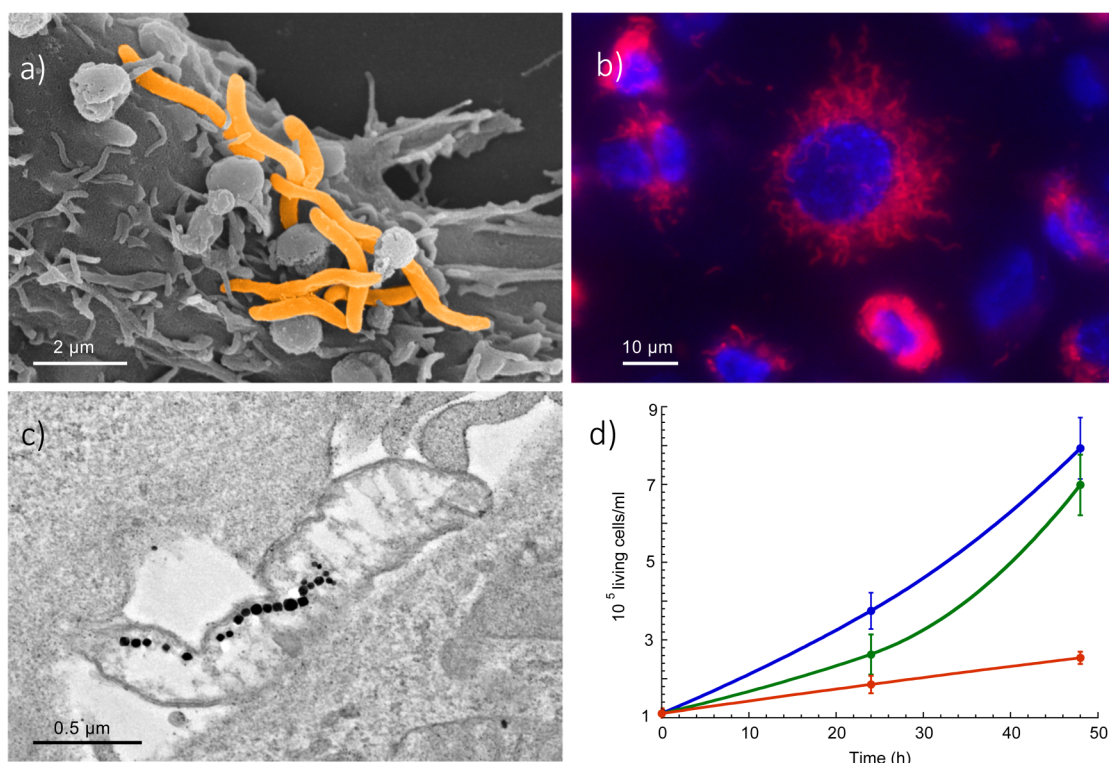


FIG. 7. Interaction of *M. gryphiswaldense* MTB with human lung A549 carcinoma cells. (a) SEM image showing MTB (in orange) adhered on the surface of A549 cells. (b) Fluorescence microscopy image of MTB bearing A549 cells. MTB were labeled with rhodamine (red) and A549 cells were stained with Hoechst (nuclei shown in blue). (c) TEM image of a cross section of A549 cells showing MTB inside the cell. (d) Time evolution of the number of live A549 cells present in the culture after the MTB uptake (in green) and after the hyperthermia treatment (in red). A control culture of cells without MTB is also shown (in blue). Reproduced with permission from Gandia *et al.*, *Small* **15**, 1902626 (2019). Copyright 2019 John Wiley & Sons.

Despite these pioneering *in vivo* experiments, the majority of the guidance and motility studies on MTB have been carried out in controlled environments, mostly in artificially patterned microfluidic channels, where the movement of the bacteria is analyzed under optical microscopy^{99–101} [Fig. 8(b)]. It has been extensively demonstrated that their trajectories can be readily controlled by an external magnetic field, being able to navigate against the rather strong opposite flow encountered in the vascular system,⁹⁹ which is of the order of 1 mm/s.¹⁰² There are, however, several other factors that must be taken into account for understanding the movement of MTB. Once those are delimited, it will be feasible to put forward a successful strategy of MTB guidance. First, understanding the interaction between MTB's two driving inputs (magnetotaxis and aerotaxis) is essential for a successful application.¹⁰³ Second, the specific way in which the movement is established is determined by the hydrodynamic interaction between their flagellar propulsion and the characteristics of the flow regime.^{104,105} Hydrodynamic and magnetic interactions can also lead to spontaneous self-organization in bacterial clusters.¹⁰⁶ This subject is intimately related to the formation and the collective control of large groups of bacteria or swarms, which are thought to increase the possibility of success in clinical treatments.¹⁰⁷ Besides, the navigation inside the ramified vascular system

presents additional challenges, such as the circumvention of obstacles encountered at bifurcations,¹⁰⁸ the interaction with other elements in the flow as red blood cells, not to mention the possible interception of the MTB by macrophages. Finally, as living entities, their use as *nanobots* must consider their individual diversity, that is, the natural differences in their development influencing, for instance, the size and maturation of the magnetosome chain, together with other circumstances that make that not all the specimens move equally, existing a significant percentage of non-motile MTB.¹⁰⁹

CHALLENGES, PERSPECTIVES, AND FUTURE SCOPE OF MTB AS CANCER THERAPY AGENTS

For the implementation of MTB in cancer therapies, a number of challenges must be addressed in the near future. Here, we will focus on three of them.

First, there is the challenge of scaling up the production of MTB and exploring synthesis tools to tune the magnetic behavior of MTB through the control of the biomineralization process of the magnetosomes. Second, MTB's greatest advantage is their self-propulsion by flagella and the possibility of controlling their movement by external fields. However, it is necessary to assess the

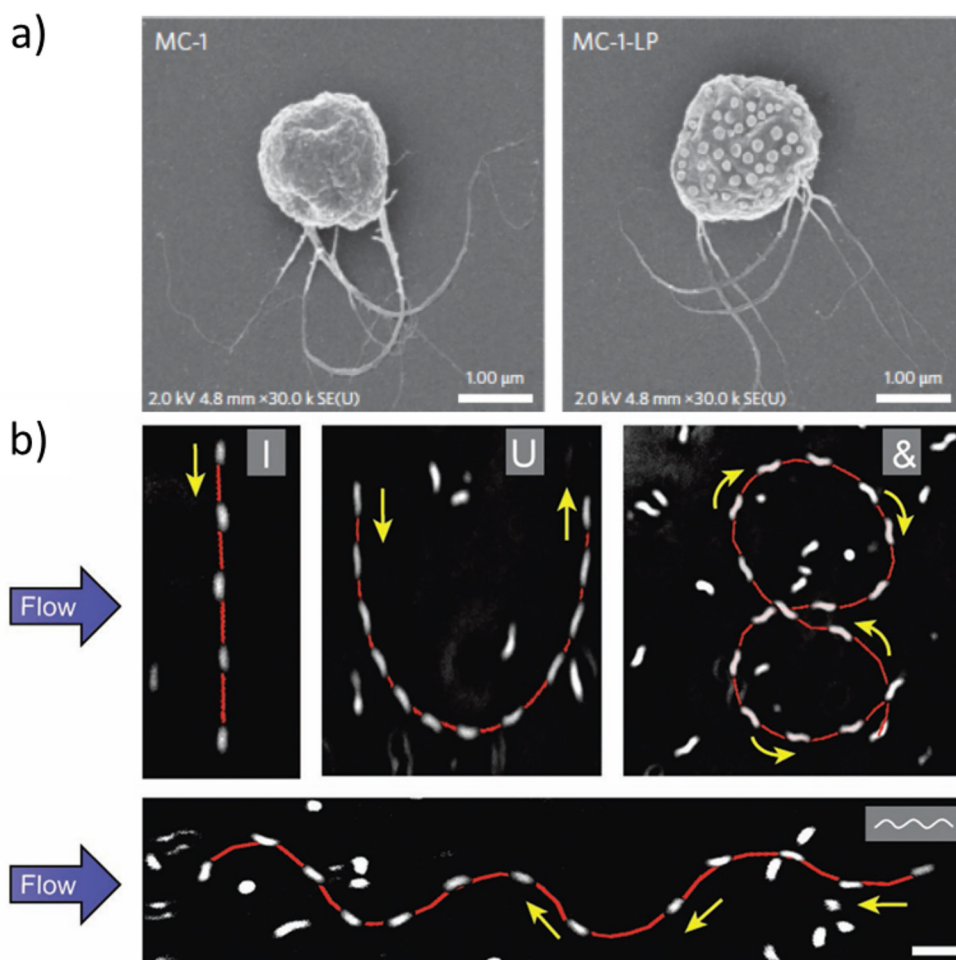


FIG. 8. (a) Scanning electron microscopy images of *M. marinus* (left) and *M. marinus* with drug-loaded liposomes (diameter, ~ 170 nm) attached to the surface of the cell (right). Reproduced with permission from Felfoul *et al.*, *Nat. Nanotechnol.* **11**, 941 (2016). Copyright 2016 Springer Nature. (b) Trajectories of directed *M. magneticum* using an applied magnetic field of 3 mT to swim along the predefined tracks in the flow with a mean velocity of $90 \mu\text{m s}^{-1}$ (shear rate of 10 s^{-1}). Predefined tracks are shown in the inset. Red lines and yellow arrows indicate the swimming trajectories and swimming directions of the bacteria, respectively. Scale bar denotes $10 \mu\text{m}$. Reproduced with permission from Rismani Yazdi *et al.*, *Small* **14**, 1702982 (2017). Copyright 2017 John Wiley & Sons.

movement capacity of the bacteria in the bloodstream, together with the penetration and distribution in the tumor. And third, the possibility of using the MTB in combination with other therapies and with diagnostic techniques should be explored.

From a production perspective, although MTB are fastidious microorganisms to grow in culture, several groups involved in the mass cultivation of MTB strains report quite high yields.^{49–54} In parallel, alternative paths are being put forward to overcome constraints associated to the scaling-up of the MTB production. One of these alternatives comes from introducing and expressing the genes involved in magnetosome formation into other bacterial species easy to grow and culture on a large-scale. This procedure has already been successfully proved in the photosynthetic model organism *Rhodospirillum rubrum*.¹¹⁰

Controlling the composition, size, and morphology of the magnetosomes during the biomineralization process is an alternative way to modify the magnetic response of MTB. While these parameters can be easily tuned in the case of inorganic MNPs, for magnetosomes this is a challenging task, since these parameters are specific to the bacterial species and are controlled by a large set of proteins present in the magnetosome membrane.^{35–38} A good understanding of all the proteins involved in the process could be the key to have a good control over these parameters through genetic engineering, although this strategy is far from being fully developed. Another route to modify the composition of magnetosomes consists on doping the magnetite with 3d transition elements. This is easily achieved by introducing salts containing 3d elements into the culture medium (for example, Co, Mn, Ni, Zn, etc.).^{111–116} The random

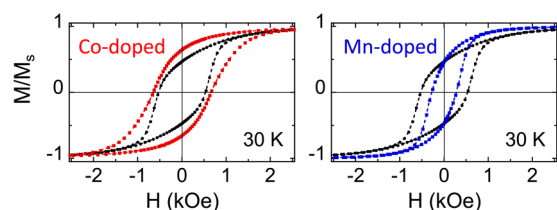


FIG. 9. Low temperature ($T = 30$ K) hysteresis loops of MTB with undoped magnetosomes (black dots) compared to MTB with: left: Co-doped (red dots); right: Mn-doped (blue dots) magnetosomes. Lines are guides for the eye. In both cases, the saturation magnetization is already reached for $H = 2.5$ kOe, but the shape of the loop is remarkably different with an evolution from hard (Co-doped) to soft (Mn-doped) magnetic behavior.

substitution of Fe cations by transition metal dopants in the magnetite structure changes the magnetic anisotropy¹¹⁵ and strongly influences the macroscopic magnetic properties of MTB as can be seen in Fig. 9. However, in all cases, the amount of dopant element internalized by magnetosomes is less than 5%, and the magnetic changes at room temperature are still small.

For hyperthermia purposes, each MTB should have as much magnetite as possible. However, the mass of magnetite per MTB typically lies around several tens of femtograms. This means that when the MTB arrive to the tumor area and penetrate inside the tumor, the MTB should proliferate until the bacterial concentration reaches 10^{11} cell/cm³ so that the concentration of magnetite is high enough for a successful hyperthermia treatment. One way to overcome this comes from increasing the number of chains and/or the number of magnetosomes per chain. These parameters are also genetically controlled and different strategies for the overexpression of magnetosomes and/or chains have been investigated,¹¹⁷ but we are far from having a good control on this issue. Another option is to apply chemical nanoengineering by attaching inorganic MNPs onto the surface of these MTB.⁹³ This is a very attractive objective for the future, although it should be explored whether these MNPs attached to the surface of the MTB affect the remote control and navigation of MTB inside the human body.

From the perspectives of targeting efficiency and distribution in the tumor area

MTBs have numerous advantages: self-propelled by flagella, magnetotaxis that allows MTB to be guided by a given path determined by an external magnetic field, aerotaxis based on MTB's preference to migrate to environments of low oxygen concentration, and the growth and proliferation of the MTB in sites of low oxygen concentration, such as those present in tumors.⁹⁸

A future challenge is to ensure that MTB can efficiently move in physiological environments.¹¹⁸ Blood flow within human capillaries can reach speeds of around 1 mm/s, definitely larger than the typical ones of MTB (up to 0.3 mm/s). Fortunately, in the tumor environment, blood flow tends to decrease due to the interstitial fluid pressure, favoring an efficient navigation.^{119,120}

Finally, it is important that these MTB become eventually degraded and excreted from the body. MTB internalized by cancer

cells have been found to be compartmentalized inside lysosomes and quickly degraded, leaving behind the magnetosome chain.⁸¹ Magnetosomes also degrade slowly over several days, maintaining persistent hyperthermal properties during this process.^{57,83} This slow degradation of the magnetosome chain would allow repeating the magnetic hyperthermia treatment for several days avoiding the injection of additional doses of MTB. On the other hand, the degradation of magnetosomes ensures that they are eventually eliminated from the human body.

Perspectives as a combined theranostic agent

It is obvious that magnetic hyperthermia has attracted most of the attention in the last few years due to the large capacity of magnetic fields to penetrate inside the human body. However, there are other alternatives for increasing localized heat through nanoparticles. In particular, photothermal therapy is based on the use of laser energy transfer to remotely heat up the nanoparticles.¹²¹ The photothermal therapy has received increasing attention in the last years, despite the concerns with laser safety and optical penetration limit. Generally, this treatment requires a lower concentration of nanoparticles and gives rise to higher heating efficiencies than the ones achieved with magnetic hyperthermia.¹²¹ Although most of the work in this area had been based on plasmonic gold and silver nanoparticles, recently different groups have revealed that iron oxide nanoparticles can also work as photothermal agents.¹²² In this line, magnetosomes have shown good results in *in vivo* cancer treatment through photothermia, with much higher cancer killing efficiency than the one solely reached with magnetic hyperthermia.⁵⁶ This has been attributed to the agglomeration of magnetosomes inside cancer cells, which does not affect their photothermal efficiency but may lower the magnetic hyperthermia. Considering these results, similar studies on the photothermal response of the whole MTB should be carried out. Likewise, a promising strategy would be to combine both magnetic hyperthermia and photothermal therapies of MTB to maximize the heating efficiency.

MTB based therapies such as magnetic hyperthermia and targeted drug delivery could be also combined with diagnostic techniques such as Magnetic Resonance Imaging (MRI) or Magnetic Particle Imaging (MPI). Regarding MRI, isolated magnetosomes have been demonstrated to show an outstanding MRI contrasting performance due to their high magnetic moment and easy functionalization, which envisages them as promising candidates for molecular imaging.^{123–125} Recently, MTB have been proposed for *in vivo* MRI monitoring of transplanted stem cells.^{126,127} On the other hand, MPI is a 3D imaging technique that allows tracking and quantifying MNPs inside the body with high spatial and temporal resolution.^{128,129} MPI is based on the non-linear magnetization response of MNPs. Recent works have already studied the potential of magnetosomes isolated from *M. gryphiswaldense* as MPI tracers.¹³⁰ Both the MRI and MPI platforms have been put forward for the combined tracking and guidance of nanorobotic magnetic agents.³

Finally, the fine implications of magnetism in the understanding of the magnetic and motility behavior of MTB is yet to be nailed in the next future. The latter will form the skeleton on which an efficient body of bio-applications should be built.

ACKNOWLEDGMENTS

The Spanish and Basque Governments are acknowledged for funding under Project Nos. MAT2017-83631-C3-R and IT-1245-19, respectively.

DATA AVAILABILITY

The data that support the findings of this study are available from the corresponding author upon reasonable request.

REFERENCES

- ¹Global Cancer Observatory, see <https://gco.iarc.fr> for information on global cancer statistics.
- ²R. P. Feynman, *Eng. Sci.* **23**, 22 (1960).
- ³S. Martel, *Biomicrofluidics* **10**, 021301 (2016).
- ⁴N. S. Forbes, *Nat. Rev. Cancer* **10**, 785 (2010).
- ⁵N. S. Forbes, R. S. Coffin, L. Deng, L. Ergin, S. Fiering, M. Giacalone, C. Gravekamp, J. L. Gulley, H. Gunn, R. M. Hoffman, B. Kaur, K. Liu, H. K. Lyerly, A. E. Marciscano, E. Moradian, S. Ruppel, D. A. Saltzman, P. J. Tattersall, S. Thorne, R. G. Vile, H. H. Zhang, S. Zhou, and G. McFadden, *J. Immunother. Cancer* **6**, 1 (2018).
- ⁶S. Zhou, C. Gravekamp, D. Bermudes, and K. Liu, *Nat. Rev. Cancer* **18**, 727 (2018).
- ⁷Q. A. Pankhurst, J. Connolly, S. K. Jones, and J. Dobson, *J. Phys. D Appl. Phys.* **36**, R167 (2003).
- ⁸N. T. K. Thanh, *Clinical Applications of Magnetic Nanoparticles: Design to Diagnosis Manufacturing to Medicine* (CRC Press, 2018).
- ⁹C. Blanco-Andujar, F. J. Teran, and D. Ortega, *Iron Oxide Nanoparticles for Biomedical Applications* (Elsevier, 2018), p. 197.
- ¹⁰Q. A. Pankhurst, N. K. T. Thanh, S. K. Jones, and J. Dobson, *J. Phys. D Appl. Phys.* **42**, 224001 (2009).
- ¹¹J. Mosayebi, M. Kiyasafar, and S. Laurent, *Adv. Healthcare Mater.* **6**, 1700306 (2017).
- ¹²MagForce AG, see <https://www.magforce.com> for information on magnetic hyperthermia clinical trials carried out at MagForce company.
- ¹³P. S. Patrick, Q. A. Pankhurst, C. Payne, T. L. Kalber, and M. F. Lythgoe, *Design and Applications of Nanoparticles in Biomedical Imaging* (Springer, Cham, 2017), pp. 1–23.
- ¹⁴Endomag, see <https://www.endomag.com> for information on tumor localization technologies developed at Endomag company.
- ¹⁵Y.-X. J. Wang, *World J. Gastroenterol.* **21**, 13400 (2015).
- ¹⁶W. T. Bull and W. B. Coley, *J. Am. Med. Assoc.* **XLIX**, 1017 (1907).
- ¹⁷R. K. Jain, *J. Clin. Oncol.* **31**, 2205 (2013).
- ¹⁸A. M. Kamat, T. W. Flaig, H. B. Grossman, B. Konety, D. Lamm, M. A. O'Donnell, E. Uchio, J. A. Efsthathiou, and J. A. Taylor, *Nat. Rev. Urol.* **12**, 225 (2015).
- ¹⁹R. W. Kasinskas and N. S. Forbes, *Cancer Res.* **67**, 3201 (2007).
- ²⁰L. A. Diaz, I. Cheong, C. A. Foss, X. Zhang, B. A. Peters, N. Agrawal, C. Bettegowda, B. Karim, G. Liu, K. Khan, X. Huang, M. Kohli, L. H. Dang, P. Hwang, A. Vogelstein, E. Garrett-Mayer, B. Kobrin, M. Pomper, S. Zhou, K. W. Kinzler, B. Vogelstein, and D. L. Huso, *Toxicol. Sci.* **88**, 562 (2005).
- ²¹J. A. Joyce and D. T. Fearon, *Cancer Immunol. Immunother.* **348**, 74 (2015).
- ²²Y. A. Yu, Q. Zhang, and A. A. Szalay, *Biotechnol. Bioeng.* **100**, 567 (2008).
- ²³S. Bellini, *Chin. J. Oceanol. Limnol.* **27**, 3 (2009).
- ²⁴R. P. Blakemore, *Science* **190**, 377 (1975).
- ²⁵C. T. Lefevre and D. A. Bazylinski, *Microbiol. Mol. Biol. Rev.* **77**, 497 (2013).
- ²⁶D. A. Bazylinski and R. B. Frankel, *Nat. Rev. Microbiol.* **2**, 217 (2004).
- ²⁷D. Faivre and D. Schuler, *Chem. Rev.* **108**, 4875 (2008).
- ²⁸D. A. Bazylinski, C. T. Lefevre, and B. H. Lower, in *Nanobiotechnology*, edited by L. L. Barton, D. A. Bazylinski, and H. Xu (Springer, New York, 2014), pp. 39–74.
- ²⁹D. A. Bazylinski, C. T. Lefevre, and D. Schuler, in *The Prokaryotes—Prokaryotic Physiology and Biochemistry*, edited by E. Rosenberg, E. F. DeLong, S. Lory, E. Stackebrandt, and F. Thompson (Springer, Berlin, 2013), pp. 453–494.
- ³⁰J. M. Thomas, E. T. Simpson, T. Kasama, and R. E. Dunin-Borkowski, *Acc. Chem. Res.* **41**, 665 (2008).
- ³¹A. M. Huizar-Félix, D. Muñoz, I. Orue, C. Magén, A. Ibarra, J. M. Barandiarán, A. Muela, and M. L. Fdez-Gubieda, *Appl. Phys. Lett.* **108**, 063109 (2016).
- ³²F. F. Guo, W. Yang, W. Jiang, S. Geng, T. Peng, and J. L. Li, *Environ. Microbiol.* **14**, 1722 (2012).
- ³³D. Muñoz, L. Marcano, R. Martín-Rodríguez, L. Simonelli, A. Serrano, A. García-Prieto, M. L. Fdez-Gubieda, and A. Muela, *Sci. Rep.* **10**, 11430 (2020).
- ³⁴F. Abreu, J. L. Martins, T. Souza Silveira, C. N. Keim, H. G. P. L. de Barros, F. J. G. Filho, and U. Lins, *Int. J. Syst. Evol. Microbiol.* **57**, 1318 (2007).
- ³⁵R. Uebe and D. Schuler, *Nat. Rev. Microbiol.* **14**, 621 (2016).
- ³⁶D. Schuler, *FEMS Microbiol. Rev.* **32**, 654 (2008).
- ³⁷A. Komeili, Z. Li, D. K. Newman, and G. J. Jensen, *Science* **311**, 242 (2006).
- ³⁸A. Komeili, H. Vali, T. J. Beveridge, and D. K. Newman, *Proc. Natl. Acad. Sci. U.S.A.* **101**, 3839 (2004).
- ³⁹M. L. Fdez-Gubieda, A. Muela, J. Alonso, A. García Prieto, L. Olivi, J. M. Barandiarán, and R. Fernández-Pacheco, *ACS Nano* **7**, 3297 (2013).
- ⁴⁰R. B. Frankel, *Annu. Rev. Biophys. Bioeng.* **13**, 85 (1984).
- ⁴¹B. H. Lower and D. A. Bazylinski, *J. Mol. Microbiol. Biotechnol.* **23**, 63 (2013).
- ⁴²R. E. Dunin-Borkowski, M. R. McCartney, R. B. Frankel, D. A. Bazylinski, M. Pósfaí, and P. R. Buseck, *Science* **282**, 1868 (1998).
- ⁴³P. Bender, L. Marcano, I. Orue, D. Alba Venero, D. Honecker, L. Fernández Barquín, A. Muela, and M. L. Fdez-Gubieda, *Nanoscale Adv.* **2**, 1115 (2020).
- ⁴⁴R. B. Frankel and R. P. Blakemore, *J. Magn. Magn. Mater.* **15–18**, 1562 (1980).
- ⁴⁵I. Orue, L. Marcano, P. Bender, A. García-Prieto, S. Valencia, M. A. Mawass, D. Gil-Cartón, D. Alba Venero, D. Honecker, A. García-Arribas, L. Fernández Barquín, A. Muela, and M. L. Fdez-Gubieda, *Nanoscale* **10**, 7407 (2018).
- ⁴⁶T. Matsunaga, T. Sakaguchi, and F. Tadakoro, *Appl. Microbiol. Biotechnol.* **35**, 651 (1991).
- ⁴⁷K. H. Schleifer, D. Schuler, S. Spring, M. Weizenegger, R. Amann, W. Ludwig, and M. Köhler, *Syst. Appl. Microbiol.* **14**, 379 (1991).
- ⁴⁸D. A. Bazylinski, T. J. Williams, C. T. Lefevre, D. Trubitsyn, J. Fang, T. J. Beveridge, B. M. Moskowitz, B. Ward, S. Schübbe, B. L. Dubbels, and B. Simpson, *Int. J. Syst. Evol. Microbiol.* **63**, 1824 (2013).
- ⁴⁹Y. Zhang, X. Zhang, W. Jiang, Y. Li, and J. Li, *Appl. Environ. Microbiol.* **77**, 5851 (2011).
- ⁵⁰A. Fernández-Castané, H. Li, O. R. T. Thomas, and T. W. Overton, *New Biotechnol.* **46**, 22 (2018).
- ⁵¹J. B. Sun, F. Zhao, T. Tang, W. Jiang, J. S. Tian, Y. Li, and J. L. Li, *Appl. Microbiol. Biotechnol.* **79**, 389 (2008).
- ⁵²K. T. Silva, P. E. Leão, F. Abreu, J. A. López, M. L. Gutarra, M. Farina, D. A. Bazylinski, D. M. G. Freire, and U. Lins, *Appl. Environ. Microbiol.* **79**, 2823 (2013).
- ⁵³Y. Liu, G. R. Li, F. F. Guo, W. Jiang, Y. Li, and L. J. Li, *Microb. Cell Fact.* **9**, 99 (2010).
- ⁵⁴I. Ali, C. Peng, Z. M. Khan, and I. Naz, *J. Basic Microbiol.* **57**, 643 (2017).
- ⁵⁵E. Alphonandéry, D. Abi Haidar, O. Seksek, F. Guyot, and I. Chebbi, *Nanoscale* **10**, 10918 (2018).
- ⁵⁶A. Plan Sangnier, S. Preveral, A. Curcio, A. K. A. Silva, C. T. Lefevre, D. Pignol, Y. Lalatonne, and C. Wilhelm, *J. Controlled Release* **279**, 271 (2018).
- ⁵⁷E. Alphonandéry, *Front Bioeng. Biotechnol.* **2**, 5 (2014).
- ⁵⁸A. Muela, D. Muñoz, R. Martín-Rodríguez, I. Orue, E. Garaio, A. Abad Díaz de Cerio, J. Alonso, J. Á. García, and M. L. Fdez-Gubieda, *J. Phys. Chem. C* **120**, 24437 (2016).
- ⁵⁹R. K. Gilchrist, R. Medel, W. D. Shorey, R. C. Hanselman, J. C. Parrott, and C. B. Taylor, *Ann. Surg.* **146**, 596 (1957).
- ⁶⁰E. A. Périgo, G. Hemery, O. Sandre, D. Ortega, E. Garaio, F. Plazaola, and F. J. Teran, *Appl. Phys. Rev.* **2**, 041302 (2015).
- ⁶¹D. Ortega Ponce and Q. Pankhurst, in *Nanoscience*, edited by P. O'Brien (Royal Society of Chemistry, 2012), pp. 60–88.

- ⁶²Q. Pankhurst, S. Jones, and J. Dobson, *J. Phys. D Appl. Phys.* **49**, 501002 (2016).
- ⁶³Y. Zhang, W. Zhang, C. Geng, T. Lin, X. Wang, L. Zhao, and J. Tang, *Prog. Nat. Sci.* **19**, 1699 (2009).
- ⁶⁴H. Gerad, D. A. Van Echo, M. Whitacre, M. Ashman, M. Helrich, J. Foy, S. Ostrow, P. H. Wiernik, and J. Aisner, *Cancer* **53**, 2585 (1984).
- ⁶⁵R. Hergt, S. Dutz, R. Müller, and M. Zeisberger, *J. Phys. Condens. Matter* **18**, S2919 (2006).
- ⁶⁶I. Andreu and E. Natividad, *Int. J. Hyperthermia* **29**, 739 (2013).
- ⁶⁷W. J. Atkinson, I. A. Brezovich, and D. P. Chakraborty, *IEEE Trans. Biomed. Eng.* **BME-31**, 70 (1984).
- ⁶⁸R. Hergt and S. Dutz, *J. Magn. Magn. Mater.* **311**, 187 (2007).
- ⁶⁹R. Das, J. Alonso, Z. Nemati Porshokouh, V. Kalappattil, D. Torres, M.-H. Phan, E. Garaio, J. Á. García, J. L. Sanchez Llamazares, and H. Srikanth, *J. Phys. Chem. C* **120**, 10086 (2016).
- ⁷⁰Z. Nemati, J. Alonso, I. Rodrigo, R. Das, E. Garaio, J. Á. García, I. Orue, M. H. Phan, and H. Srikanth, *J. Phys. Chem. C* **122**, 2367 (2018).
- ⁷¹Z. Nemati, J. Alonso, L. M. Martinez, H. Khurshid, E. Garaio, J. A. Garcia, M.-H. Phan, and H. Srikanth, *J. Phys. Chem. C* **120**, 8370 (2016).
- ⁷²D. Gandia, L. Gandarias, L. Marcano, I. Orue, D. Gil-Cartón, J. Alonso, A. García-Arribas, A. Muela, and M. L. Fdez-Gubieda, *Nanoscale* **12**, 16081 (2020).
- ⁷³N. A. Usov and J. M. Barandiarán, *J. Appl. Phys.* **112**, 053915 (2012).
- ⁷⁴J. M. Byrne, V. S. Coker, S. Moise, P. L. Wincott, D. J. Vaughan, F. Tuna, E. Arenholz, G. van der Laan, R. A. D. Patrick, J. R. Lloyd, and N. D. Telling, *J. R. Soc. Interface* **10**, 20130134 (2013).
- ⁷⁵N. A. Usov, *J. Appl. Phys.* **107**, 123909 (2010).
- ⁷⁶S. Laurent, S. Dutz, U. O. Häfeli, and M. Mahmoudi, *Adv. Colloid Interface Sci.* **166**, 8 (2011).
- ⁷⁷C. Martínez-Boubeta, K. Simeonidis, A. Makridis, M. Angelakeris, O. Iglesias, P. Guardia, A. Cabot, L. Yedra, S. Estradé, F. Peiró, Z. Saghi, P. A. Midgley, I. Conde-Leborán, D. Serantes, and D. Baldomir, *Sci. Rep.* **3**, 1652 (2013).
- ⁷⁸M. Ma, Y. Wu, J. Zhou, Y. Sun, Y. Zhang, and N. Gu, *J. Magn. Magn. Mater.* **268**, 33 (2004).
- ⁷⁹J. Carrey, B. Mehdaoui, and M. Respaud, *J. Appl. Phys.* **109**, 083921 (2011).
- ⁸⁰N. A. Usov and S. E. Peschany, *J. Magn. Magn. Mater.* **174**, 247 (1997).
- ⁸¹D. Gandia, L. Gandarias, I. Rodrigo, J. Robles-García, R. Das, E. Garaio, J. Á. García, M. H. Phan, H. Srikanth, I. Orue, J. Alonso, A. Muela, and M. L. Fdez-Gubieda, *Small* **15**, 1902626 (2019).
- ⁸²R. Le Fèvre, M. Durand-Dubief, I. Chebbi, C. Mandawala, F. Lagroix, J. P. Valet, A. Idbaih, C. Adam, J. Y. Delattre, C. Schmitt, C. Maake, F. Guyot, and E. Alphanféry, *Theranostics* **7**, 4618 (2017).
- ⁸³R. Liu, J. Liu, J. Tong, T. Tang, W.-C. Kong, X. Wang, Y. Li, and J. Tang, *Prog. Nat. Sci. Mater. Int.* **22**, 31 (2012).
- ⁸⁴E. Alphanféry, I. Chebbi, F. Guyot, and M. Durand-Dubief, *Int. J. Hyperthermia* **29**, 801 (2013).
- ⁸⁵E. Alphanféry, S. Faure, O. Seksek, F. Guyot, and I. Chebbi, *ACS Nano* **5**, 6279 (2011).
- ⁸⁶E. Alphanféry, A. Idbaih, C. Adam, J. Y. Delattre, C. Schmitt, F. Guyot, and I. Chebbi, *Biomaterials* **141**, 210 (2017).
- ⁸⁷E. Alphanféry, A. Idbaih, C. Adam, J. Y. Delattre, C. Schmitt, F. Gazeau, F. Guyot, and I. Chebbi, *J. Nanobiotechnol.* **17**, 126 (2019).
- ⁸⁸D. Chang, M. Lim, J. A. C. M. Goos, R. Qiao, Y. Y. Ng, F. M. Mansfeld, M. Jackson, T. P. Davis, and M. Kavallaris, *Front. Pharmacol.* **9**, 831 (2018).
- ⁸⁹H. S. Huang and J. F. Hainfeld, *Int. J. Nanomed.* **8**, 2521 (2013).
- ⁹⁰A. J. Clark, D. T. Wiley, J. E. Zuckerman, P. Webster, J. Chao, J. Lin, Y. Yen, and M. E. Davis, *Proc. Natl. Acad. Sci. U.S.A.* **113**, 3850 (2016).
- ⁹¹M. Molcan, H. Gojzewski, A. Skumiel, S. Dutz, J. Kovac, M. Kubovcikova, P. Kopcansky, L. Vekas, and M. Timko, *J. Phys. D Appl. Phys.* **49**, 365002 (2016).
- ⁹²E. Alphanféry, S. Faure, L. Raison, E. Dugué, P. A. Howse, and D. A. Bazylinski, *J. Phys. Chem. C* **115**, 18 (2011).
- ⁹³M. S. Tabatabaei, H. Girouard, and S. Martel, in *International Conference on Manipulation, Automation and Robotics at Small Scales, MARSS 2017—Proceeding* (Institute of Electrical and Electronics Engineers Inc., 2017), pp. 1–5.
- ⁹⁴N. A. Usov and B. Y. Liubimov, *J. Appl. Phys.* **112**, 023901 (2012).
- ⁹⁵C. Chen, L. Chen, Y. Yi, C. Chen, L. F. Wu, and T. Song, *Appl. Environ. Microbiol.* **82**, 2219 (2016).
- ⁹⁶J. Riegler, K. D. Lau, A. García-Prieto, A. N. Price, T. Richards, Q. A. Pankhurst, and M. F. Lythgoe, *Med. Phys.* **38**, 3932 (2011).
- ⁹⁷M. R. Benoit, D. Mayer, Y. Barak, I. Y. Chen, W. Hu, Z. Cheng, S. X. Wang, D. M. Spielman, S. S. Gambhir, and A. Martin, *Clin. Cancer Res.* **15**, 5170 (2009).
- ⁹⁸O. Felfoul, M. Mohammadi, S. Taherkhani, D. de Lanauze, Y. Zhong Xu, D. Loghin, S. Essa, S. Jancik, D. Houle, M. Lafleur, L. Gaboury, M. Tabrizian, N. Kaou, M. Atkin, T. Vuong, G. Batist, N. Beauchemin, D. Radzioch, and S. Martel, *Nat. Nanotechnol.* **11**, 941 (2016).
- ⁹⁹S. Rismani Yazdi, R. Nosrati, C. A. Stevens, D. Vogel, P. L. Davies, and C. Escobedo, *Small* **14**, 1702982 (2018).
- ¹⁰⁰I. S. M. Khalil, M. P. Pichel, B. A. Reefman, O. S. Sukas, L. Abelmann, and S. Misra, in *Proceedings—IEEE International Conference on Robotics and Automation* (IEEE, 2013), Vol. 5508.
- ¹⁰¹M. P. Pichel, T. A. G. Hageman, I. S. M. Khalil, A. Manz, and L. Abelmann, *J. Magn. Magn. Mater.* **460**, 340 (2018).
- ¹⁰²P. E. Bunney, A. N. Zink, A. A. Holm, C. J. Billington, and C. M. Kotz, *Physiol. Behav.* **176**, 139 (2017).
- ¹⁰³A. Codutti, K. Bente, D. Faivre, and S. Klumpp, *PLoS Comput. Biol.* **15**, e1007548 (2019).
- ¹⁰⁴C. J. Pierce, E. Mumper, E. E. Brown, J. T. Brangham, B. H. Lower, S. K. Lower, F. Y. Yang, and R. Sooryakumar, *Phys. Rev. E* **95**, 062612 (2017).
- ¹⁰⁵N. Waisbord, C. T. Lefèvre, L. Bocquet, C. Ybert, and C. Cottin-Bizonne, *Phys. Rev. Fluids* **1**, 53203 (2016).
- ¹⁰⁶C. J. Pierce, H. Wijesinghe, E. Mumper, B. H. Lower, S. K. Lower, and R. Sooryakumar, *Phys. Rev. Lett.* **121**, 188001 (2018).
- ¹⁰⁷J. Yu, B. Wang, X. Du, Q. Wang, and L. Zhang, *Nat. Commun.* **9**, 3260 (2018).
- ¹⁰⁸S. Rismani Yazdi, R. Nosrati, C. A. Stevens, D. Vogel, and C. Escobedo, *Biomicrofluidics* **12**, 011101 (2018).
- ¹⁰⁹S. Klumpp, B. Kiani, P. Vach, and D. Faivre, *Phys. Scr.* **T165**, 014044 (2015).
- ¹¹⁰I. Kolinko, A. Lohße, S. Borg, O. Raschdorf, C. Jogler, Q. Tu, M. Pósfai, E. Tompa, J. M. Pitzko, A. Brachmann, G. Wanner, R. Müller, Y. Zhang, and D. Schüler, *Nat. Nanotechnol.* **9**, 193 (2014).
- ¹¹¹T. Prozorov, T. Perez-Gonzalez, C. Valverde-Tercedor, C. Jimenez-Lopez, A. Yebra-Rodriguez, A. Körnig, D. Faivre, S. K. Mallapragada, P. A. Howse, D. A. Bazylinski, R. Prozorov, “Manganese incorporation into the magnetosome magnetite: Magnetic signature of doping,” *Eur. J. Mineral.* **26**(4), 457–471 (2014).
- ¹¹²E. Alphanféry, C. Carvallo, N. Menguy, and I. Chebbi, *J. Phys. Chem. C* **115**, 11920 (2011).
- ¹¹³L. Marcano, D. Munoz, R. Martín-Rodríguez, I. Orue, J. Alonso, A. García-Prieto, A. Serrano, S. Valencia, R. Abrudan, L. Fernández Barquín, A. García-Arribas, A. Muela, and M. L. Fdez-Gubieda, *J. Phys. Chem. C* **122**, 7541 (2018).
- ¹¹⁴S. Staniland, W. Williams, N. Telling, G. Van Der Laan, A. Harrison, and B. Ward, *Nat. Nanotechnol.* **3**, 158 (2008).
- ¹¹⁵M. Tanaka, R. Brown, N. Hondow, A. Arakaki, T. Matsunaga, and S. Staniland, *J. Mater. Chem.* **22**, 11919 (2012).
- ¹¹⁶J. Li, N. Menguy, M. A. Arrio, P. Sainctavit, A. Juhin, Y. Wang, H. Chen, O. Bunau, E. Otero, P. Ohresser, and Y. Pan, *J. R. Soc. Interface* **13**, 20160355 (2016).
- ¹¹⁷A. Lohße, I. Kolinko, O. Raschdorf, R. Uebe, S. Borg, A. Brachmann, J. M. Pitzko, R. Müller, Y. Zhang, and D. Schüler, *Appl. Environ. Microbiol.* **82**, 3032 (2016).
- ¹¹⁸M. Luo, Y. Feng, T. Wang, and J. Guan, *Adv. Funct. Mater.* **28**, 1706100 (2018).
- ¹¹⁹D. De Lanauze, O. Felfoul, J. P. Turcot, M. Mohammadi, and S. Martel, *Int. J. Rob. Res.* **33**, 359 (2014).
- ¹²⁰N. Mokrani, O. Felfoul, F. Fatemeh Afkhami, M. Mohammadi, R. Aloyz, G. Batist, and S. Martel, in *32nd Annual International Conference on IEEE EMBS* (IEEE, 2010), pp. 4371–4374.

- ¹²¹D. Jaque, L. Martínez Maestro, B. del Rosal, P. Haro-Gonzalez, A. Benayas, J. L. Plaza, E. Martín Rodríguez, and J. García Solé, *Nanoscale* **6**, 9494 (2014).
- ¹²²M. Chu, Y. Shao, J. Peng, X. Dai, H. Li, Q. Wu, and D. Shi, *Biomaterials* **34**, 4078 (2013).
- ¹²³S. Mériaux, M. Boucher, B. Marty, Y. Lalatonne, S. Prévéral, L. Motte, C. T. Lefèvre, F. Geffroy, F. Lethimonnier, M. Péan, D. Garcia, G. Adryanczyk-Perrier, D. Pignol, and N. Ginet, *Adv. Healthcare Mater.* **4**, 1076 (2015).
- ¹²⁴Z. Xiang, X. Yang, J. Xu, W. Lai, Z. Wang, Z. Hu, J. Tian, L. Geng, and Q. Fang, *Biomaterials* **115**, 53 (2017).
- ¹²⁵M. Boucher, F. Geffroy, S. Prévéral, L. Bellanger, E. Selingue, G. Adryanczyk-Perrier, M. Péan, C. T. Lefèvre, D. Pignol, N. Ginet, and S. Mériaux, *Biomaterials* **121**, 167 (2017).
- ¹²⁶J. H. Jung, Y. Tada, and P. C. Yang, in *Biological, Physical and Technical Basics of Cell Engineering*, edited by G. M. Artmann, A. Artmann, A. A. Zhubanova, and I. Digel (Springer, Singapore, 2018), pp. 365–380.
- ¹²⁷M. Mahmoudi, A. Tachibana, A. B. Goldstone, Y. J. Woo, P. Chakraborty, K. R. Lee, C. S. Foote, S. Piecewicz, J. C. Barrozo, A. Wakeel, B. W. Rice, C. B. Bell, and P. C. Yang, *Sci. Rep.* **6**, 1 (2016).
- ¹²⁸B. Gleich and J. Weizenecker, *Nature* **435**, 1214 (2005).
- ¹²⁹X. L. C. Wu, X. Y. Zhang, X. G. Steinberg, X. H. Qu, X. S. Huang, X. M. Cheng, X. T. Bliss, X. F. Du, X. J. Rao, X. G. Song, X. L. Pisani, X. T. Doyle, X. S. Conolly, X. K. Krishnan, X. G. Grant, and X. M. Wintermark, *Am. J. Neuroradiol.* **40**, 206 (2019).
- ¹³⁰A. Kraupner, D. Eberbeck, D. Heinke, R. Uebe, D. Schüller, and A. Briel, *Nanoscale* **9**, 5788 (2017).